Mon. Not. R. Astron. Soc. **000**, 1–?? (2012) Printed 21 November 2012 (MN LATEX style file v2.2)

He II optical depth and UV escape fraction of galaxies

Vikram Khaire⋆ and Raghunathan Srianand†
IUCAA, Post Bag 4, Pune, India - 411007

ABSTRACT

We study the effect of H I ionizing photons escaping from the high-z galaxies on the He II ionizing ultraviolet background (UVB) radiation. We show, while these photons do not directly interact with He II ions, they play an important role through radiative transport in modifying the shape of He II ionizing part of UVB spectrum. Within the observed range of UV escape from galaxies, we show the rapid increase in He II Ly α effective optical depth at $z \sim 2.7$ can be naturally explained without resorting to pre-overlap era of He II reionization. Therefore, a well measured He II Ly α effective optical depth vs z relationship can be used to constrain the redshift evolution of UV escape from high-z galaxies. Our study also stresses the importance of including galaxy contribution even in the fluctuating UV background calculations.

Key words: Cosmology:theory – intergalactic medium – diffuse radiation

1 INTRODUCTION

The spectroscopy of $z \geqslant 6$ QSOs (Fan et al. 2006) and cosmic microwave background (CMB) polarization observations (Larson et al. 2011) suggest that H I in intergalactic medium (IGM) got reionized at $6 \leqslant z \leqslant 12$. The reionized IGM at $z \leqslant 6$ is believed to be in ionization equilibrium with UVB emanating from QSOs and galaxies (Haardt & Madau 2012, HM12 hereafter). Measured temperature of the IGM at $z \leqslant 3$ (Becker et al. 2011), claimed excess temperature around $z \sim 6$ QSOs (Bolton et al. 2012), lack of substantial contribution to E > 54.4 eV photons from galaxies and redshift distribution of QSOs (Hopkins et al. 2007) all favor He II reionization occurring over $2.5 \leqslant z \leqslant 6.0$.

Direct measurements of He II Ly-α absorption from IGM is possible towards few UV bright high-z QSOs using Hubble space telescope (for summary of observations see, Shull et al. 2010). The cosmic-variance limited available data suggest a rapid evolution of He II Ly-α effective optical depth ($\tau_{\alpha,\rm HeII}$) and large fluctuation in the column density ratio of He II and H I (called as η) over $2.7 \leqslant z \leqslant 3.0$. The rapid evolution of the $\tau_{\alpha,\rm HeII}$ is attributed to the completion of He II reionization at this epoch (Furlanetto & Oh 2008; McQuinn et al. 2009). The large fluctuation in η over small scales can be attributed to (i) small number of bright QSOs within a typical mean free path ($\lambda_{\rm mfp}$) of He II ionizing photons (Fardal et al. 1998; Furlanetto 2009); (ii) large scatter in the QSO spectral index (Shull et al. 2004); (iii) presence of collisionally ionized gas (Muzahid et al. 2011) and (iv) small scale radiative transport effects (Maselli & Ferrara 2005). Most of the theoretical calculations of He II optical depth consider only the QSO emissivity and radiative transport assuming the IGM gas in photoionization equilibrium. While galaxies do not contribute directly to the He II ionizing radiation they can influence the ionization state of the IGM gas thereby affecting the He II optical depth. Here, we explore this using a cosmological radiative transfer code similar to HM12. We show that the $\lambda_{\rm mfp}$ is very sensitive to escape fraction ($f_{\rm esc}$) of H I ionizing photons from galaxies and the redshift evolution of $\tau_{\alpha,\rm HeII}$ can be used to constrain $f_{\rm esc}$ from high-z galaxies. Details of our calculations assuming (Ω_m,Ω_Λ,h)=(0.3, 0.7, 0.7) cosmology is given in the following section.

2 UVB CALCULATION

We calculated the UV background spectrum contributed by QSOs and galaxies using the standard assumption that each volume element is an isotropic emitter and sink (see for example, Haardt & Madau 1996; Fardal et al. 1998; Faucher-Giguère et al. 2009). The angle and space averaged specific intensity J_{ν_0} (in units of erg cm^{-2} s^{-1} Hz^{-1} sr^{-1}) of diffuse UV background as seen by an observer at a redshift z_0 and frequency ν_0 is given by (Haardt & Madau 1996):

$$J_{\nu_0}(z_0) = \frac{1}{4\pi}\int_{z_0}^{\infty} dz\, \frac{dl}{dz}\, \frac{(1+z_0)^3}{(1+z)^3}\, \epsilon_\nu(z)\, e^{-\tau_{\rm eff}(\nu_0,\, z_0,\, z)}\,, \quad (1)$$

where $\nu = \nu_0(1+z)/(1+z_0)$ is the frequency of emitted radiation at redshift z, $\epsilon_\nu(z)$ is the proper space averaged specific volume emissivity of radiating sources (QSOs and galaxies), $\frac{dl}{dz}$ is the proper line element in the Friedmann-Robertson-Walker cosmology and $\tau_{\rm eff}$ is the effective optical depth which quantifies the attenuation of photons observed

⋆ E-mail: vikramk@iucaa.ernet.in
† E-mail: anand@iucaa.ernet.in

at a frequency ν_0 while travelling through the IGM in between z and z_0.

If we assume that the IGM clouds with neutral hydrogen column density, $N_{\rm HI}$, are Poisson-distributed along the line of sight, we can write $\tau_{\rm eff}$ as (Paresce et al. 1980),

$$\tau_{\rm eff}(\nu_0, z_0, z) = \int_{z_0}^{z} dz' \int_0^{\infty} dN_{\rm HI} \frac{\partial^2 N}{\partial N_{\rm HI}\, \partial z'} (1 - e^{-\tau(\nu')}) \,, \quad (2)$$

where, $f(N_{\rm HI}, z) = \partial^2 N / \partial N_{\rm HI} \partial z$, is the number of absorbers with $N_{\rm HI}$ per unit redshift and column density interval measured at z. This is directly measured with QSO spectroscopy (see Petitjean et al. 1993). Assuming that absorbing clouds are made up of a pure H and He gas, the continuum optical depth through an individual cloud can be written as,

$$\tau(\nu') = N_{\rm HI}\sigma_{\rm HI}(\nu') + N_{\rm HeI}\sigma_{\rm HeI}(\nu') + N_{\rm HeII}\sigma_{\rm HeII}(\nu') \,. \quad (3)$$

Here, $\nu' = \nu_0(1+z')/(1+z_0)$ and N_x and σ_x are the column density and photoionization cross-section for a species x respectively. From QSO spectroscopy we know $N_{\rm HeI}$ is negligible when $N_{\rm HI} \leqslant 10^{17.2}$ cm^{-2}. Even for Lyman limit systems ($N_{\rm HI} > 10^{17.2}$ cm^{-2}), the ratio $N_{\rm HeI}/N_{\rm HI}$ is small (see HM12) enough to neglect its contribution over the redshift range of interest in our study. Therefore, Eq. (3) becomes

$$\tau(\nu) \approx N_{\rm HI}[\sigma_{\rm HI}(\nu) + \eta\, \sigma_{\rm HeII}(\nu)]. \quad (4)$$

In the absence of direct measurements of $f(N_{\rm HeII}, z)$, a knowledge of η as a function of $N_{\rm HI}$ together with $f(N_{\rm HI}, z)$ allows us to calculate the contribution of He II to the continuum optical depth. Under photoionization equilibrium the $N_{\rm HI}$ and $N_{\rm HeII}$ are related through the following quadratic equation (Fardal et al. 1998; Faucher-Giguère et al. 2009; Haardt & Madau 2012),

$$\frac{n_{\rm He}}{4n_{\rm H}} \frac{I_{\rm HI}\ \tau_{912,\rm HI}}{(1 + {\rm A}\ \tau_{912,\rm HI})} = \tau_{228,\rm HeII} + \frac{I_{\rm HeII}\ \tau_{228,\rm HeII}}{(1 + {\rm B}\ \tau_{228,\rm HeII})} \quad (5)$$

where, $\tau_{\lambda,x}$ is $N_x\sigma_x(\lambda)$ for the species x. The values of A and B depend on the assumed relationship between the total hydrogen column density ($N_{\rm H}$) and electron density (n_e). This relationship is obtained for a constant density slab of gas with a thickness of Jeans length under optically thin photoionization equilibrium (Schaye 2001). Numerical simulations suggest that such a relationship is valid for log $N_{\rm H}\leqslant$18 (see Rahmati et al. 2012). We have considered a series of photoionization models of plane parallel slab having $N_{\rm H}$-n_e relationship of Schaye (2001) illuminated by a powerlaw source using the photoionization code Cloudy (see Ferland et al. 1998). We confirm that the values A = 0.02 and B = 0.25 (as used by HM12) provide a good fit to the model predictions and adopt these values in our calculations. The quantity I_x for $x^{\rm th}$ species is defined as $I_x = \Gamma_x/n_e\alpha_x({\rm T})$, where $\alpha_x({\rm T})$ is the case-A recombination coefficient and Γ_x is photoionization rate of $x^{\rm th}$ species as given by,

$$\Gamma_x = \int_{\nu_x}^{\infty} d\nu\, 4\pi\, \frac{J_\nu}{h\nu}\, \sigma_x(\nu) \,. \quad (6)$$

Here ν_x is the ionization threshold frequency for the species x. We use T = 2×10^4 K and the form of n_e and $f(N_{\rm HI}, z)$ as given in HM12 in all our calculations.

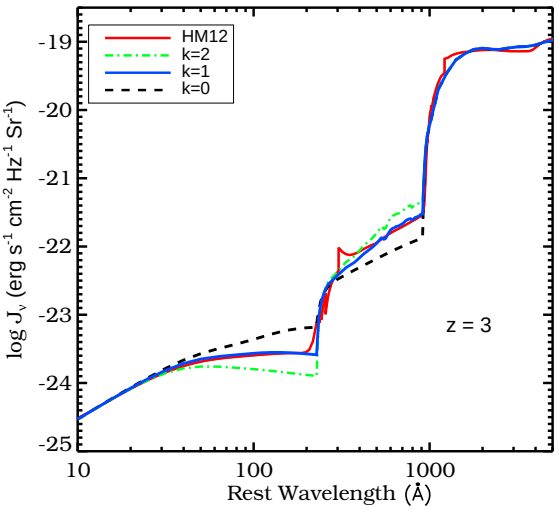

Figure 1. UV background spectrum at $z = 3$ from our models for different values of k. The spectrum plotted in red is from HM12.

2.1 Quasar and Galaxy emissivity

The specific volume emissivity of radiating sources, $\epsilon_\nu(z)$, is a sum of the emissivity from galaxies, $\epsilon_{\nu,{\rm G}}(z)$, and quasars, $\epsilon_{\nu,{\rm Q}}(z)$. We have considered the parametric form to the observed quasar co-moving emissivity at 912Å as given in HM12,

$$\frac{\epsilon_{912,{\rm Q}}(z)}{(1+z)^3} = 10^{24.6}\,(1+z)^{4.68}\,\frac{exp(-0.28z)}{exp(1.77z) + 26.3} \quad (7)$$

in units of ergs Mpc^{-3} s^{-1} Hz^{-1} together with the broken power law spectral energy distribution (SED), $L_\nu \propto \nu^{-0.44}$ for λ >1300Å and $L_\nu \propto \nu^{-1.57}$ for λ <1300Å (Vanden Berk et al. 2001; Telfer et al. 2002). To calculate the co-moving emissivity from galaxies we have taken the parametric form of star formation rate density (SFRD) used in HM12 :

$${\rm SFRD}(z) = \frac{6.9\times10^{-3} + 0.14(z/2.2)^{1.5}}{1 + (z/2.7)^{4.1}}\ {\rm M_\odot yr^{-1} Mpc^{-3}}. \quad (8)$$

The co-moving emissivity of galaxies (in units ergs Mpc^{-3} s^{-1} Hz^{-1}) is taken to be,

$$\frac{\epsilon_{\nu,{\rm G}}(z)}{(1+z)^3} = C(z) \times {\rm SFRD}(z) \times l_\nu(z, {\rm Z}) \,. \quad (9)$$

Here, $l_\nu(z, {\rm Z})$ is the specific luminosity of a galaxy produced for every solar mass of gas having metallicity Z being converted to stars. We get $l_\nu(z, {\rm Z})$ using the stellar population synthesis model 'Starburst99 v6.0.3' (Leitherer et al. 1999) for Z=0.001 and Salpeter initial mass function with stellar mass range 0.1 to 100 M$_\odot$. SED fitting studies, semi-analytic modelling of luminosity function and spatial clustering are consistent with star formation in a typical galaxy lasting for a few 100 Myr (see discussions in Jose et al. 2012, and references there in). Therefore, for simplicity we assume that the star formation has lasted for more than 100 Myr. This assumption allows us to get a linear relationship between star formation rate and luminosity. We do not

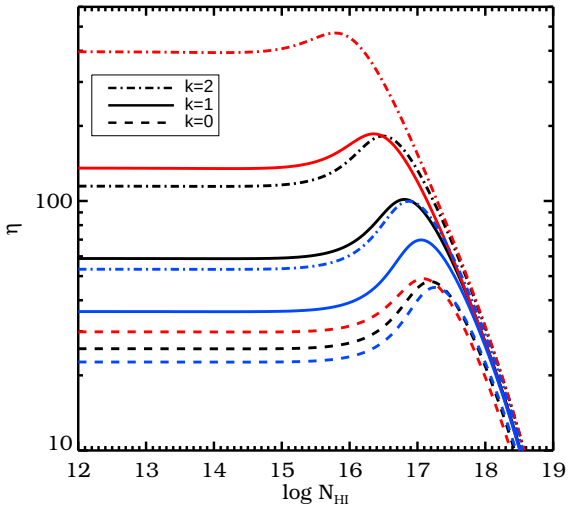

Figure 2. η as a function of N_{HI} for redshifts 2 (*blue*), 2.5 (*black*) and 3 (*red*). The dash, solid and dot-dash curves are for $k = 0$, 1 and 2 respectively.

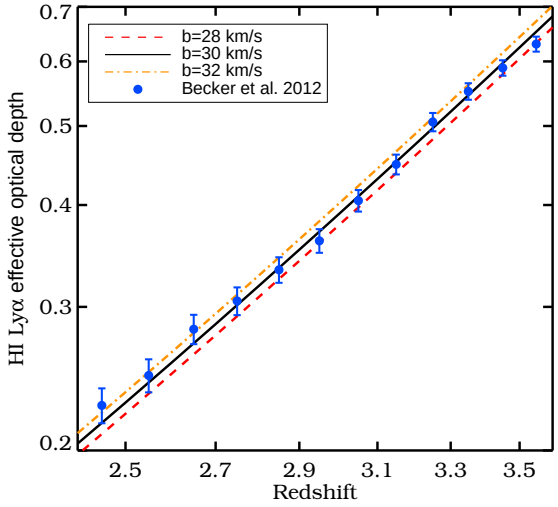

Figure 3. H I Lyα effective optical depth as a function of z for different values of b parameters. The observed points are from Becker et al. (2012).

include recombination emissivity and resonant absorption effects in our calculations.

The factor $C(z)$ is used to modify the SED to take care of the reddening and UV escape. For λ >912Å, $C(z)$ is $exp(-\tau_\nu)$ with τ_ν being the frequency dependent dust optical depth calculated using extinction law of Calzetti et al. (2000) with $R_V = 3.1$. The dust correction may depend on the luminosity and z of individual galaxies (see for example Bouwens et al. 2012). However, for simplicity we use a single value at all z. The dust optical depth is chosen to have a reddening correction factor of 3 at 1500Å.

For wavelength range 228Å< λ <912Å we take $C(z) = f_{\rm esc}$. To take into account the redshift evolution in the $f_{\rm esc}$ found by Inoue et al. (2006) we adopt the form of HM12 and use,

$$C(z) = f_{\rm esc} = k\ [3.4 \times 10^{-4}(1+z)^{3.4}]\ . \qquad (10)$$

In this case $C(z)$ corresponds to the absolute escape fraction, $f_{\rm esc}$, defined as the ratio of escaping Lyman continuum (LyC) flux from a galaxy to the one which is intrinsically produced by the stars in it (Leitherer et al. 1995) and k is a free parameter that allows us to change the values of $f_{\rm esc}$. For our fiducial star formation model, at $k = 1$ we get UV emissivity from galaxies similar to that of HM12. Models with $k = 0$ corresponds to spectrum contributed by QSOs alone at λ <912Å. Note, no reddening correction is applied for λ < 912Å and we simply scale the unattenuated spectrum by $f_{\rm esc}$. In other words, we assume all the ionizing photons that are escaping through holes in the galaxy. We take $C(z) = 0$ for λ <228Å because galaxies at the redshifts of our interest do not produce sufficient He II ionizing photons as massive Population-III stars are rare.

3 RESULTS AND DISCUSSION

In Fig. 1, we present the UVB spectrum at $z = 3$ computed using our numerical code for three different k values. At $z = 3$, $k = 1$ and 2 corresponds to $f_{\rm esc}$ of ∼4% and ∼8% respectively. This is well within the inferred range for high-z galaxies and Ly-α emitters at $z \sim 3$ (Shapley et al. 2006; Iwata et al. 2009; Boutsia et al. 2011; Nestor et al. 2012). The range of $\Gamma_{-12,\rm HI} = 0.4 - 1.3$ predicted by our models is also consistent with the range allowed by the observations (see, Meiksin & White 2004; Bolton & Haehnelt 2007; Faucher-Giguère et al. 2008). For comparison we also plot the UVB spectrum generated by HM12. It is clear that our model with $k = 1$ reproduces HM12 spectrum very well. The differences in $\Gamma_{\rm HI}$ and $\Gamma_{\rm HeII}$ between the two codes is much less than the spread in these values due to allowed range in $f_{\rm esc}$. It is clear from Fig. 1 that increasing (decreasing) k increases (decreases) $\Gamma_{\rm HI}$ and decreases (increases) $\Gamma_{\rm HeII}$. As $\lambda \leqslant$228Å emissivity is not affected by galaxies, the variation of $\Gamma_{\rm HeII}$ with $f_{\rm esc}$ can be attributed to the effect of $f_{\rm esc}$ on He II opacity. Below we explore this in more detail.

3.1 Escape fraction and η

In Fig. 2 we have plotted η vs. $N_{\rm HI}$ at redshift 2, 2.5 and 3 for different k values. Two trends are clearly evident for $\log N_{\rm HI} \leqslant 17$: (i) for any given $f_{\rm esc}$, η increases with increasing z and (ii) at any z, η increases with increasing $f_{\rm esc}$. The first trend can be understood in a simple way for the optically thin limit where $\eta \propto \Gamma_{\rm HI}/\Gamma_{\rm HeII}$. Both QSOs and galaxies contribute to $\Gamma_{\rm HI}$ but to $\Gamma_{\rm HeII}$ only QSOs alone contribute. Therefore, η depends on how population of QSO and galaxy evolve with redshift. For $z \geqslant 2.5$, population of QSOs declines rapidly (Ross et al. 2012) while that of galaxies remains almost same (Bouwens et al. 2011) helping η to increase. However, at any z by increasing $f_{\rm esc}$, we are increasing the galaxy contribution to $\Gamma_{\rm HI}$ which will further increase η. This explains the second trend we notice in Fig. 2. *A simple physical picture we can draw is, a given $N_{\rm HI}$ is produced by integrating over larger column length when*

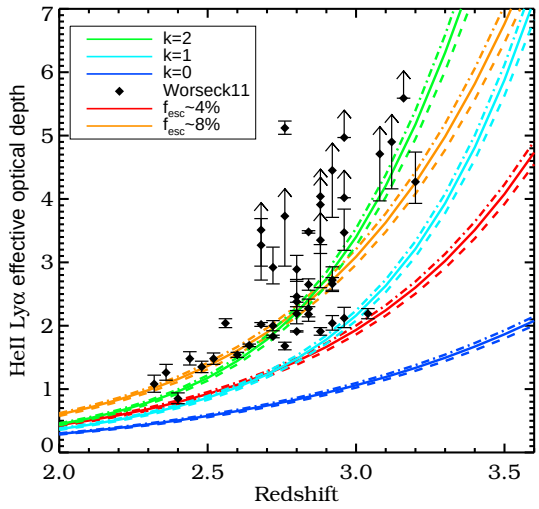

Figure 4. Lyα effective optical depth for He II as a function of redshift for different $f_{\rm esc}$ and b parameters ($b = 28$ *dash curve*, $b = 30$ *solid curve*, $b = 32$ *dot dash curve*) in km/s. Black diamonds are observations of Worseck et al. (2011).

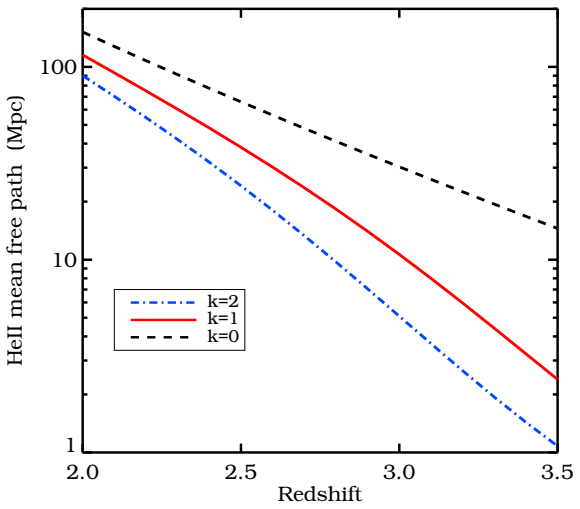

Figure 5. Mean free path for He II ionizing photons as a function of z for different k values. Here, distance is in proper length scale.

$\Gamma_{\rm HI}$ *is high and therefore we get more* $N_{\rm HeII}$. However, the implied ionization corrections for the range of $f_{\rm esc}$ considered here still keeps Ω_b within the allowed range from CMB observations.

3.2 Ly α effective optical depth for H I and He II

Now we estimate the Ly α effective optical depth of H I (i.e., $\tau_{\alpha,\rm HI}$) and He II (i.e., $\tau_{\alpha,\rm HeII}$) for a range of $f_{\rm esc}$ and compare with the available observations. The $\tau_{\alpha,\rm HI}$ and $\tau_{\alpha,\rm HeII}$ is given by (Paresce et al. 1980; Madau & Meiksin 1994),

$$\tau_{\alpha,x}(z) = \frac{1+z}{\lambda_{\alpha,x}} \int_0^\infty dN_{\rm HI}\, f(N_{\rm HI}, z)\, W_{\rm n}\ , \qquad (11)$$

where, $\lambda_{\alpha,x}$ is 1215.67Å for H I , 303.78Å for He II and $W_{\rm n}$ is equivalent width of corresponding line expressed in wavelength units given by,

$$W_{\rm n} = \int_0^\infty d\lambda\, (1 - e^{-y\phi(\lambda)})\ . \qquad (12)$$

Here $y = N_{\rm HI}$ for H I , $y = \eta\, N_{\rm HI}$ for He II and $\phi(\lambda)$ is Voigt profile function. In Fig. 3, we show our best fit to the observed $\tau_{\alpha,\rm HI}$ vs z relationship (Becker et al. 2012) obtained for b parameter values $b = 30 \pm 2$ kms^{-1}.

In Fig. 4, we have plotted $\tau_{\alpha,\rm HeII}$ vs. z for different $f_{\rm esc}$ values along with observations of Worseck et al. (2011). Here, we assume that the non-thermal motions dominate the He II line broadening and used the best fit values of b obtained for H I. In all cases $\tau_{\alpha,\rm HeII}$ increases with increasing z. However the rate of increase depends on $f_{\rm esc}$. Interestingly, a sharp raising trend of $\tau_{\alpha,\rm HeII}$ at $z \sim 3$, seen for $k = 1$, almost provides a lower envelop to the observations. For $k = 2$, the model prediction almost passes through most of the observed mean points at $z \leqslant 2.7$. This means that $f_{\rm esc}$ can not be much higher than 8% in this redshift range. To check whether the rapid rise in $\tau_{\alpha,\rm HeII}$ is a consequence of $(1+z)^{3.4}$ evolution assumed for $f_{\rm esc}$ (Eq. 10), in Fig.4 we also plot the $\tau_{\alpha,\rm HeII}$ computed for redshift independent $f_{\rm esc}$ (i.e 4% and 8%). Even in these cases, the z evolution of $\tau_{\alpha,\rm HeII}$ is more steeper than for $k = 0$. This observed rise and scatter in $\tau_{\alpha,\rm HeII}$ is usually attributed to the pre-overlap era of He III bubbles assuming that the He II re-ionization completes around $z = 2.7$ (Dixon & Furlanetto 2009; Shull et al. 2010; Worseck et al. 2011). *Our results suggest that the observed trend of* $\tau_{\alpha,\rm HeII}$ *with* z *can also be produced naturally by the radiative transfer effects associated with changing* $f_{\rm esc}$. Also a well measured lower envelop of $\tau_{\alpha,\rm HeII}$ with z can be used to constrain the redshift evolution of $f_{\rm esc}$.

Next we calculate the $\lambda_{\rm mpf}$ predicted by our models. We define,

$$\lambda_{\rm mfp} = \left|\frac{dl}{dz}\right| \quad \frac{dz}{d\tau_{\rm eff}}\ , \qquad (13)$$

where from Eq. (2) we write,

$$\frac{d\tau_{\rm eff}}{dz} = \int_0^\infty {\rm dN_{HI}}\, f(N_{\rm HI},\, z)\left[1 - e^{-\tau(228\text{Å})}\right]\ . \qquad (14)$$

Here, $\tau(228\text{Å}) = {\rm N_{HI}}(\sigma_{\rm HI,228Å} + \eta\sigma_{\rm HeII,228Å})$. In Fig. 5 the $\lambda_{\rm mfp}$ of He II ionizing photons is plotted as a function of z for different $f_{\rm esc}$. These curves are well approximated by $\lambda_{\rm mpf}(z) = A_1 \times exp[-(z-2)/\Delta z]$ with best fit values of A_1=[150, 120, 90] Mpc and Δz=[0.60, 0.41, 0.37] respectively for k=[0,1,2]. This clearly demonstrates the rapid reduction in $\lambda_{\rm mpf}$ with $f_{\rm esc}$. This is a consequence of the fact that when we increase $f_{\rm esc}$, a given $N_{\rm HeII}$ is produced by a cloud with lower $N_{\rm HI}$ (i.e η increases). As $f(N_{\rm HI}, z)$ is powerlaw in $N_{\rm HI}$ with a negative slope the $\lambda_{\rm mfp}$ reduces steeply. For our fiducial model with $k = 1$, $\lambda_{\rm mfp}$ is 22 and 11 proper Mpc at $z = 2.7$ and 3.0 respectively. These are at least a factor 2 smaller than the corresponding values for $k = 0$.

Recently, Davies & Furlanetto (2012) have computed the mean evolution of $\tau_{\alpha,\rm HeII}$ assuming diffuse emissivity of QSOs and allowing for fluctuating $\Gamma_{\rm HeII}$. This model also produces a rapidly evolving $\tau_{\alpha,\rm HeII}$ with z without implicitly assuming He II reionization around $z \sim 3$ when a minimum $\lambda_{\rm mfp}$ of 35 comoving Mpc is used. This is already more than

$\lambda_{\rm mfp}$ we get at $z = 3$ for our fiducial model. Therefore, we can conclude that the galaxy contribution, that is usually ignored, will play an important role in fluctuation calculations. We also speculate that the redshift at which the fluctuations beginning to dominate will also depend on $f_{\rm esc}$. Detailed investigations of high ionization species like N V and O VI absorption in QSO spectra at $z \geqslant 2.5$ and proximity effect analysis of He II Ly-α forest will provide more insights into the issues discussed here. We plan to address these carefully in near future.

4 CONCLUSIONS

We studied the effect of escape fraction of H I ionizing photons from high-z galaxies on the UVB calculated by solving cosmological radiative transfer equation. We have demonstrated that the H I ionizing photons from galaxies play an important role in deciding the shape of He II ionizing part of UVB and affect the transmission of UVB through IGM. The main results are summarized below : (i) He II ionizing part of UVB depends strongly on the value of $f_{\rm esc}$ for $z > 2.0$. This is a consequence of the dependence of ratio $\eta = N_{\rm HeII}/N_{\rm HI}$ on $f_{\rm esc}$. (ii) Mean free path of He II ionizing photons decreases rapidly with increasing $f_{\rm esc}$. Suggesting the fluctuations in η can be much higher compared to the one computed ignoring the galaxy contributions. (iii) We show for the range of $f_{\rm esc}$ allowed by the observations the rapid increase in He II Lyα effective optical depth, recently observed at $z \sim 2.7$, can be naturally explained without invoking pre-overlapping era of He II re-ionization around this redshift. Thus one will be able to place strong constraints on $f_{\rm esc}$ as a function of z using effective optical depth evolution of He II . We also show the observations at $z \leqslant 2.7$ are consistent with $f_{\rm esc}$ being not much higher than 8%.

ACKNOWLEDGMENTS

We wish to thank T. R. Choudhury and K. Subramanian for useful discussions. VK thanks CSIR for providing support for this work.

REFERENCES

Becker G. D., Bolton J. S., Haehnelt M. G., Sargent W. L. W., 2011, MNRAS, 410, 1096
Becker G. D., Hewett P. C., Worseck G., Prochaska J. X., 2012, arXiv:1208.2584
Bolton J. S., Haehnelt M. G., 2007, MNRAS, 382, 325
Bolton J. S., Becker G. D., Raskutti S., Wyithe J. S. B., Haehnelt M. G., Sargent W. L. W., 2012, MNRAS, 419, 2880
Boutsia K. et al., 2011, ApJ, 736, 41
Bouwens R. J. et al., 2011, Natur, 469, 504
Bouwens R. J. et al., 2012, ApJ, 754, 83
Calzetti D., Armus L., Bohlin R. C., Kinney A. L., Koornneef J., Storchi-Bergmann T., 2000, ApJ, 533, 682
Davies F. B., Furlanetto S. R., 2012, arXiv:1209.4900
Dixon K. L., Furlanetto S. R., 2009, ApJ, 706, 970
Fan X. et al., 2006, AJ, 132, 117
Fardal M. A., Giroux M. L., Shull J. M., 1998, AJ, 115, 2206
Faucher-Giguère C. A., Prochaska J. X., Lidz A., Hernquist L., Zaldarriaga M., 2008, ApJ, 681, 831
Faucher-Giguère C. A., Lidz A., Zaldarriaga M., Hernquist L., 2009, ApJ, 703, 1416
Ferland G. J., Korista K. T., Verner D. A., Ferguson J. W., Kingdon J. B., Verner E. M., 1998, PASP, 110, 761
Furlanetto S. R., 2009, ApJ, 703, 702
Furlanetto S. R., Oh S. P., 2008, ApJ, 681, 1
Haardt F., Madau P., 1996, ApJ, 461, 20
Haardt F., Madau P., 2012, ApJ, 746, 125
Hopkins P. F., Richards G. T., Hernquist L., 2007, ApJ, 654, 731
Inoue A. K., Iwata I., Deharveng J. M., 2006, MNRAS, 371, L1
Iwata I. et al., 2009, ApJ, 692, 1287
Jose C., Subramanian K., Srianand R., Samui S., 2012, arXiv:1208.2097
Larson D. et al., 2011, ApJS, 192, 16
Leitherer C., Ferguson H. C., Heckman T. M., Lowenthal J. D., 1995, ApJ, 454, L19
Leitherer C. et al., 1999, ApJS, 123, 3
Madau P., Meiksin A., 1994, ApJ, 433, L53
Maselli A., Ferrara A., 2005, MNRAS, 364, 1429
McQuinn M., Lidz A., Zaldarriaga M., Hernquist L., Hopkins P. F., Dutta S., Faucher-Giguère C. A., 2009, ApJ, 694, 842
Meiksin A., White M., 2004, MNRAS, 350, 1107
Muzahid S., Srianand R., Petitjean P., 2011, MNRAS, 410, 2193
Nestor D. B., Shapley A. E., Kornei K. A., Steidel C. C., Siana B., 2012, ArXiv e-prints
Paresce F., McKee C. F., Bowyer S., 1980, ApJ, 240, 387
Petitjean P., Webb J. K., Rauch M., Carswell R. F., Lanzetta K., 1993, MNRAS, 262, 499
Rahmati A., Pawlik A. P., Raičević M., Schaye J., 2012, arXiv:1210.7808
Ross N. P. et al., 2012, arXiv:1210.6389
Schaye J., 2001, ApJ, 559, 507
Shapley A. E., Steidel C. C., Pettini M., Adelberger K. L., Erb D. K., 2006, ApJ, 651, 688
Shull J. M., Tumlinson J., Giroux M. L., Kriss G. A., Reimers D., 2004, ApJ, 600, 570
Shull J. M., France K., Danforth C. W., Smith B., Tumlinson J., 2010, ApJ, 722, 1312
Telfer R. C., Zheng W., Kriss G. A., Davidsen A. F., 2002, ApJ, 565, 773
Vanden Berk D. E. et al., 2001, AJ, 122, 549
Worseck G. et al., 2011, ApJ, 733, L24